Available online at www.sciencedirect.com
SCIENCE DIRECT®
Acta Materialia 52 (2004) 1589–1595
Acta MATERIALIA
www.actamat-journals.com

Substrate-induced supramolecular ordering of functional molecules: theoretical modelling and STM investigation of the PEBA/Ag(1 1 1) system

M. Vladimirova [a,*], G. Trimarchi [b,c], A. Baldereschi [a], J. Weckesser [d,e], K. Kern [d,e], J.V. Barth [d], A. De Vita [b,c,f,g]

[a] *Institut Romand de Recherche Numérique en Physique des Matériaux (IRRMA), PPH-Ecublens, 1015 Lausanne, Switzerland*
[b] *Dipartimento di Ingegneria dei Materiali, Università di Trieste, via A. Valerio 2, 34127 Trieste, Italy*
[c] *INFM-DEMOCRITOS National Simulation Center, Trieste, Italy*
[d] *Institut de Physique des Nanostructures, Ecole Politechnique Fédérale de Lausanne, 1015 Lausanne, Switzerland*
[e] *Max Planck Institute für Ferstköperforschung, Heisenbergstasse 1, D-70569 Stuttgart, Germany*
[f] *Department of Physics, King's College London, Strand, London WC2R 2LS, UK*
[g] *Center of Excellence for Nanostructured Materials, Trieste, Italy*

Received 29 April 2003; received in revised form 2 December 2003; accepted 3 December 2003

Abstract

We model the geometry, binding site and absolute orientation of the self-assembled monolayer of 4-[pyrid-4-yl-ethynyl] benzoic acid (PEBA) adsorbed on the (1 1 1) surface of silver by means of molecular dynamics and first principles calculations, and compare these results with those we obtain from scanning tunneling microscopy experiments. Our results indicate that the adsorbate–substrate interaction controls the overall orientation of the self-assembled molecular superstructures. We investigate the nature of this interaction, which is found to induce some degree of readjustment of the molecular structure and substantial stretching of the intermolecular hydrogen bonds. This is consistent with the nodal structure of the interaction-induced ab initio differential charge density, which can be interpreted in terms of a simple extended Hückel model.

Keywords: Molecular adsorption; Hydrogen bonding; Ab initio calculations; STM; Self-assembly

1. Introduction

Understanding at the atomic level the properties of 2D self-assembled materials consisting of organic layers adsorbed on support surfaces is of fundamental interest, and may soon be relevant for technology. The use of highly controlled growth techniques in conjunction with the scanning tunneling microscopy (STM) tools [1,2] and electronic structure based modern materials modelling techniques [3] makes these systems readily accessible to direct investigation at the fundamental level. Research on high quality thin films, with a controlled nanometer-size thickness, structure, morphology, and purity is also stimulated by the goal to obtain self-assembled materials structures with well defined properties and functionalities. Several applications in the molecular electronics domain have been proposed based on supramolecular engineering [4]. Also, nonlinear optics applications can be realized using stiff planar molecules with uneven charge distribution as building blocks for supramolecular hydrogen-bonded films [5]. The adsorption and self-assembly of such molecules on a substrate is driven by a delicate interplay between molecule–molecule and molecule–substrate interaction. It is, thus, important to evaluate the relative contribution of these driving forces to understand what causes the observed supramolecular arrangement.

* Corresponding author.
E-mail address: vladimirova@ges.univ-montp2.fr (M. Vladimirova).

1359-6454/$30.00 © 2003 Acta Materialia Inc. Published by Elsevier Ltd. All rights reserved.
doi:10.1016/j.actamat.2003.12.004

In this paper, we study the 4-[pyrid-4-yl-ethynyl] benzoic acid (PEBA) self-assembly on the (1 1 1) surface of silver. This fairly rigid, planar rode-like molecule consists of a pyridyl group and carboxylic acid moiety connected by an ethynylene bridge [6] (see Fig. 1). The inhomogeneous distribution of charge within the molecule induces the electrostatic potential depicted in Fig. 1, with a negative region associated with the molecular tail and a positive region in correspondence of the proton in the COOH group. Therefore, one can expect substantial attractive interactions involving head-to-tail hydrogen bonds [6,7], possibly producing chain-like linkages between PEBA molecules, upon adsorption on the surface [8]. Indeed, STM experiments show that the PEBA molecules are adsorbed in a planar geometry and assemble in 2D enantiometric islands [9], as discussed in Section 2 . Despite the asymmetry of the carboxylic acid moiety, no fixed chirality is associated to the individual molecules adsorbed on the surface. This is because the "asymmetric" hydrogen atom on COOH is expected to be able to move from one oxygen atom to another, in analogy with related systems [8,10]. Recently, a model has been proposed to interpret the observed PEBA arrangement on the Ag(1 1 1) surface [9]. The proposed head-to-tail bonded periodic structure is in good agreement with the experimental images.

In this work, we perform large-scale first principles calculations in which the metal surface is explicitely represented, and compare the results with experimental observations to investigate the role of the substrate in determining the self-assembled structures. So far, it has been assumed that this role is simply limited to that of a planar constraint for the self-assembly process. Remarkably, however, we find that the equilibrium supramolecular arrangement would differ from the experimentally observed structure if this were the case. In other words, even if the strength of the inter-molecular bonding is very significant compared to the roughness of the physisorption potential, the interaction with the substrate is strong enough to determine some *qualitative features* of the self-assembled structure. The effects of the substrate consist mainly of inter-molecular hydrogen bonds length stretching, and in a slight deformation of the molecules upon adsorption on the surface. Another important issue is that of explaining the experimental orientation of the molecular superstructure along the low symmetry $[3\,\bar{1}\,\bar{2}]$ directions of the Ag(1 1 1) surface. Here the observations contrast with what is found in superstructures formed by very similar molecular species on the same substrate [8,9]. The comparison between the equilibrium molecular stride in the observed PEBA monolayer (ML) and the atomic distances in the Ag(1 1 1) surface layer reveals that the selection of the $[3\,\bar{1}\,\bar{2}]$ direction and its rotationally equivalent directions is due to the interplay between molecule–substrate and inter-molecular interactions including *lateral bonding* in the ML. Furthermore, using ab initio total energy calculations we identify the preferential adsorption geometry for the PEBA molecules in the ML, and provide an estimate for the corrugation of the adsorption potential. Finally, the binding energy of the ML on the surface is compared with the cohesive energy of a molecule in a ML reported in [9] and the molecule–substrate interaction is discussed in terms of molecular orbitals hybridization.

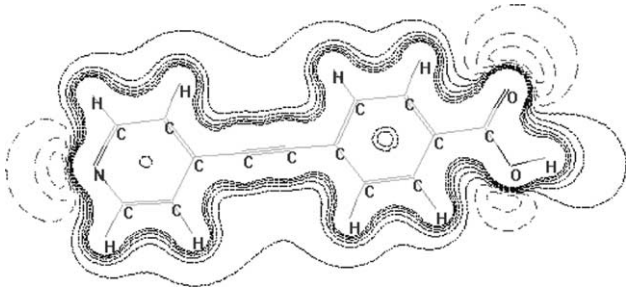

Fig. 1. Electrostatic potential of an isolated PEBA molecule; solid and dashed lines are associated to positive and negative potential regions.

The paper is organized as follows: Experimental procedure and results are presented in Section 2. Section 3 contains a description of our theoretical calculations. The first subsection is devoted to PEBA structures in vacuum, while the second one describes a first principles study of PEBA adsorption on the Ag(1 1 1) surface. Section 4 summarizes the results.

2. Experimental results

The Ag(1 1 1) surfaces are prepared by repeated argon ion sputtering and subsequent annealing at 870 K, which account for an atomically clean substrate with large terraces. The molecules are then deposited by organic vapor phase epitaxy. The so obtained films are annealed at room temperature and the prepared samples are transferred in the home-built low temperature STM. All of our measurements are performed after quenching the samples down to 77 K (see [9] for further details). Fig. 2 shows a STM image of a large surface area crossed by several monatomic steps. Wide terraces appear almost completely covered with molecules while low local coverage is observed on smaller terraces, where only steps are decorated. This indicates: (i) that the molecules can easily migrate over the step edges; (ii) that the growth proceeds from island formation on terraces, rather than from 1D molecular rows formed at step edges.

The step edge decoration has been observed in a variety of molecule-on-metal systems [11] and is usually ascribed to the Smoluchowski effect [12]. In this work we will concentrate on the 2D island structures. From high resolution STM data (Fig. 3(a)) one can derive the

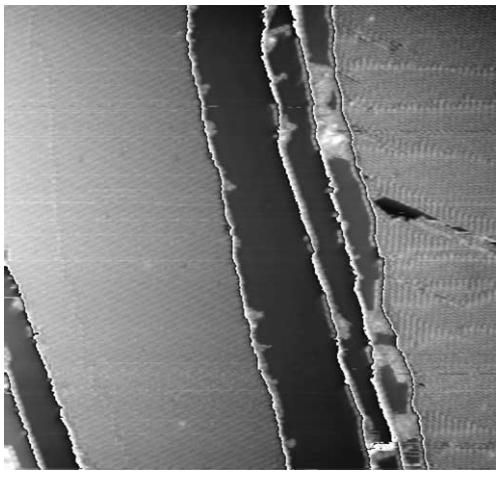

Fig. 2. Large scale STM image of PEBA on Ag(1 1 1), crossed by several monoatomic steps. The large terraces are filled by molecules, while on the small ones only step edges are decorated.

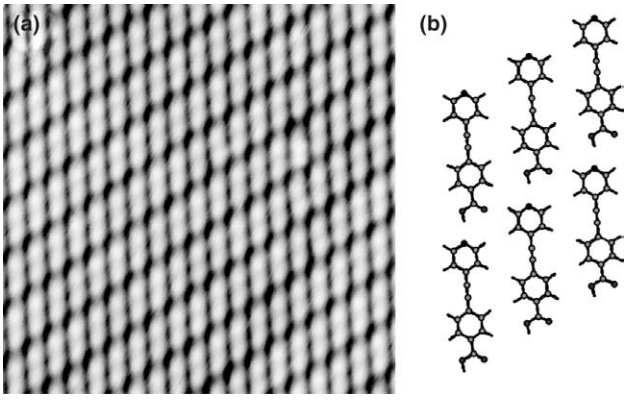

Fig. 3. (a) High resolution STM image of a PEBA island on Ag(1 1 1) (detail). (b) Proposed model for the arrangement of PEBA molecules in the island, after [9].

structural model proposed in [9] (Fig. 3(b)). The islands are well ordered periodic enantiomorphic structures constructed from head-to-tail hydrogen bonded molecular chains, shifted with respect to one another and laterally linked by one CH···OC bound per chain segment.

Detailed analysis reveals that the molecular axis is rotated ~5° clockwise with respect to the chain orientation. This arrangement corresponds to the optimal geometry in the head-to-tail linkage between the adjacent endgroups. The molecular chains are oriented along the $[3\,\bar{1}\,\bar{2}]$ and its two rotationally equivalent directions, reflecting the symmetry of the Ag(1 1 1) surface. Due to the mirror symmetry of the substrate, each orientation corresponds to two observed domains of molecular assembly related by a mirror operation, having opposite chirality. Thus, a total of six different domains are observed on the surface. The periodicity (''stride'') of the PEBA chains measured from the STM images is ~15.3 Å with inter-row distance d of ~6.6 Å. Assuming that the molecules are arranged according to the model of [9] (Fig. 3(b)), the distance between the ''head'' O and the ''tail'' N atoms is ~2.35 Å (corresponding to a calculated 0.45 eV cohesive energy per PEBA molecule in the ML). The STM results and these values leave some questions open. For instance, the 2.35 Å length of the OH···N bond is much higher than the typical hydrogen bond length 1.5–1.7 Å reported in literature for the same bonding type in 3D organic crystals [13]. This suggest a possible role of the substrate in determining the stride of PEBA chains, so that it would be interesting to get some insight in the adsorption energy and in the roughness of the adsorption potential energy surface. Also, it resulted impossible to resolve experimentally the Ag atoms underlying the molecules, so that the exact position of the molecule with respect to the surface, i.e., the stable adsorption geometry, is not known. Thus, the problem of determining the stable geometry and strength of the molecule–surface interaction is addressed theoretically in the following.

3. Model calculations and results

The main tool adopted in the present work is the ab initio total energy approach to Computational Materials Science (see [3] for an extended review). The approach is based on the density functional theory (DFT) within the generalized gradient approximation (GGA) [14] for supramolecular structures and local density approximation (LDA) [15] for structures including metallic slabs. We note that the GGA approximation is known to be more accurate than LDA in the description of hydrogen bonds [16]. However, the debate on whether this is also the case for molecules adsorbed on metal surfaces, in particular for modelling dispersive interactions in molecular physisorption is still open [17,18]. We use a supercell approach in periodic boundary conditions, and expand the electronic wave functions and the electron density on plane-wave basis sets up to kinetic energy cut-offs of 50 and 200 Ry, respectively. We adopt the Car–Parrinello method [20] to optimize the electronic and ionic structure, using the Γ-point to sample the Brillouin Zone (BZ) associated to the simulation cells. The norm-conserving Troullier–Martins pseudopotentials [19] are used to represent the interaction between valence electrons and core ions.

We apply the scheme proposed in [21] to treat metallic systems, using a smearing energy $E_s = 0.25$ eV to smooth the Fermi level discontinuity. In all the calculations the atomic positions are relaxed (except for the atoms of the lowermost layer of the silver slab, which are kept fixed at their ideal bulk positions) until all residual force components are smaller than 0.03 eV/Å. These techniques have been recently applied in a series

of total energy calculations in a similar system consisting of 1-nitronaphtalene (NN) molecules adsorbed on the Au(1 1 1) [22]. Test calculations reported in [22] show that good cancellation of the errors originating from finite supercell size and BZ sampling can be expected in evaluating energy differences.

Our molecular dynamics (MD) simulations of the PEBA self-assembly are carried out using a classical force field (FF) constructed from ab initio electrostatic potential of an isolated molecule. In this approach the molecules, which are assumed to move rigidly, are represented as a set of point charges located on the atoms. These "partial Coulomb" charges are determined from the best fit of the isolated molecule DFT electrostatic potential in the region outside a Van der Waals (VDW) exclusion area, defined by optimized VDW radii of 3.8, 3.6, 3.3 and 2.9 Å for C, N, O and H atoms, respectively [23]. The electrostatic contribution of the underlying metal surface is included in the force field by means of a simple image charge scheme [22]. Similar force fields have been successfully applied to a variety of hydrogen bonded systems [1]. Tests reveal that the OH···N bond length in the PEBA dimer structure (discussed in detail below) obtained using these force fields differ by less then 0.01 Å from their ab initio values.

3.1. Gas phase calculations

The starting point of our analysis is the PEBA head-to-tail dimer, which is the basic element for molecular islands formation. We first use the FF model to produce a realistic initial dimer configuration and then use the latter as input in an ab initio calculation. We choose a $39.7\times11.9\times11.9$ Å^3 ab initio supercell, sufficiently big to rule out spurious interactions between repeated images. After full atomic relaxation, we obtain a OH···N bond length of 1.72 Å and a binding energy of 0.52 eV for the gas-phase dimer in the planar geometry (see Fig. 4). These results are consistent with known hydrogen bond properties [13]. However, the calculated bond length is much smaller than the value 2.35 Å measured in the STM images of adsorbed PEBA monolayers. This suggests that some further effect originates from the adsorbate–substrate interaction, as discussed below.

To get insight in the PEBA islands geometry, we follow the procedure used in [9], i.e., we investigate PEBA "gas phase" monolayer geometries imposing the

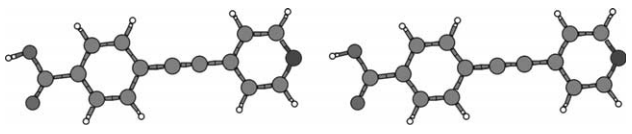

Fig. 4. PEBA head-to-tail dimer geometry after full atomic relaxation.

($\sqrt{7}\times2\sqrt{7}$) $R(\arctan\sqrt{3}/5)$ translational symmetry observed on the Ag substrate (cf. Fig. 3(b)), here not specifically included. We use the 4.05 Å LDA lattice parameter for silver to determine the unit cell 15.15×7.57 Å size in the xy plane, while the cell height is set to 10 Å in the z-direction perpendicular to the layer. We use the LDA lattice parameter, slightly smaller than the experimentally measured 4.08 Å used in [9], to facilitate further comparison of this isolated ML structure with the ML adsorbed on the metal surface addressed in LDA calculations described below. The calculation gives a OH···N bond length 2.26 Å, a value again slightly smaller than the GGA result (2.35 Å). A similar effect is obtained for the total molecular length, whose values are 12.88 and 12.94 Å in LDA and GGA calculations, respectively. We note, however, that the *bonding geometry* of the ML calculated in the framework of the LDA is not affected by these numerical changes, so that the stereochemical reasoning of [9] applies identically to the present work.

3.2. Monolayer of PEBA on Ag(1 1 1) surface

From the geometry in vacuum of the PEBA dimers obtained in Section 3.1, we can extract an indicative value 14.6 Å for what would be the optimal stride of the molecular rows in the ML arrangement in the absence of adsorption potential corrugation. Considering the best fit of this length with the substrate periodicity along the various possible crystallographic directions on the Ag(1 1 1) surface, we can try to rationalize the preferential orientation of the PEBA ML with respect to the substrate. Surprisingly, the best matching of the PEBA chain stride with the Ag(1 1 1) surface would be achieved along the $[1\,1\,\bar{2}]$ direction, which would imply a 15.0 Å stride, and not along the experimentally observed $[3\,\bar{1}\,\bar{2}]$ direction, whose periodicity is 15.3 Å. Thus, the observed orientation of the PEBA monolayer cannot be simply explained by considering the optimal stretching of the head-to-tail hydrogen bond only. At the same time, it appears that *lateral* interactions between PEBA chains arranged along the high symmetry $[1\,1\,\bar{2}]$ direction are very unfavorable. Indeed, the Ag(1 1 1) substrate cannot provide a better stride than 10 Å in the $[\bar{2}\,1\,1]$ direction, that is along the other surface cell unit vector direction, which is rotated by 120° with respect to the $[1\,1\,\bar{2}]$. Therefore, the lateral interaction between chains oriented along the $[1\,1\,\bar{2}]$ direction cannot be reconciled with any commensurate positioning of the PEBA ML on the underlying atomic layer substrate. On the contrary, the observed $[\bar{2}\,3\,\bar{1}]$ chain direction allows for a 7.64 Å experimental stride for the lateral bonding, with a corresponding CH···O lateral bond length of 2.52 Å. Thus, we conclude that the orientation of the ML with respect to the surface is driven by inter- and intra-chain molecular bonding, which is modified upon

adsorption to provide the best commensurate match with the substrate.

We now address the position of the single molecule with respect to the substrate. To identify the PEBA adsorption site, we performed four independent calculations starting from four different PEBA initial arrangements at fixed supercell size. We note that PEBA is complex enough a molecule that it would be impractical to explore the whole spectrum of its possible ML arrangements on the Ag(1 1 1) substrate even though the orientation of the ML (i.e., the direction of the *chains*) is known. The oxygen and nitrogen being the most reactive atoms, we fix the initial molecular position by placing these free atoms on high symmetry sites of the fcc metal substrate. The resulting starting positions are shown in Fig. 5, the initial distance between the molecule and the surface being set to 3.0 Å. The total energy of each local minimum structure is obtained by full electronic and structural relaxation starting from here.

In these calculations, the silver slab contains four atomic layers and the cell dimension in the *z*-direction is set to 19.51 Å, so that the slab is separated from its repeated image by 10 Å of vacuum. The relevant quantities we are interested in are energy differences between the various adsorption geometries under study, both to identify the stable adsorption geometry and to estimate the strength of the coupling between the monolayer geometry and the substrate. We find that the stable adsorption geometry is the one shown in Fig. 5(a). From the differences in binding energies between the configurations under study (see Fig. 5), we estimate the amplitude of the substrate corrugation potential to be ~0.3 eV. A side view of the relaxed stable system is shown in Fig. 6. This geometry is associated to a non-negligible relaxation of the molecule with respect to its initial configuration. Indeed, the pyridyl group is about 0.1 Å closer to the surface than the benzoic acid moiety

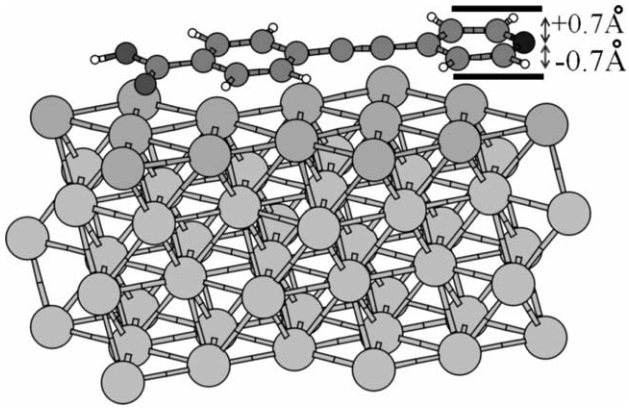

Fig. 6. Simulated system representing the PEBA monolayer on Ag(1 1 1), after full atomic relaxation of the lowest energy structure. The cut planes corresponding to Fig. 7 are shown.

in the relaxed structure, while the average molecule–substrate distance shrinks to 2.7 Å. Concerning the molecule position on the *xy* plane, a tendency to arrange both oxygen atoms on "atop" sites is apparent, while nitrogen keeps its initial position. Moreover, the ML molecules are stretched up to 13.00 Å (to be confronted with 12.82 Å for an isolated molecule and 12.88 Å for the gas phase PEBA ML), so that the OH···N hydrogen bond is reduced to 2.16 Å, a value inferior to the 2.26 Å one found for the unsupported PEBA ML but still significantly longer than the 1.72 Å OH···N bond length obtained for the planar gas-phase dimer.

To summarize, in order to match the Ag(1 1 1) surface the ML of PEBA appears to deform substantially. The energy cost of the PEBA ML deformation comes mainly from the elongation of the molecules (i) and OH···N intermolecular bonds (ii). To estimate the energy related to the bond stretching (ii) we perform a couple of GGA total energy calculations of a single PEBA chain in the gas phase. The corresponding unit cells contain two molecules interacting via 2.16 and

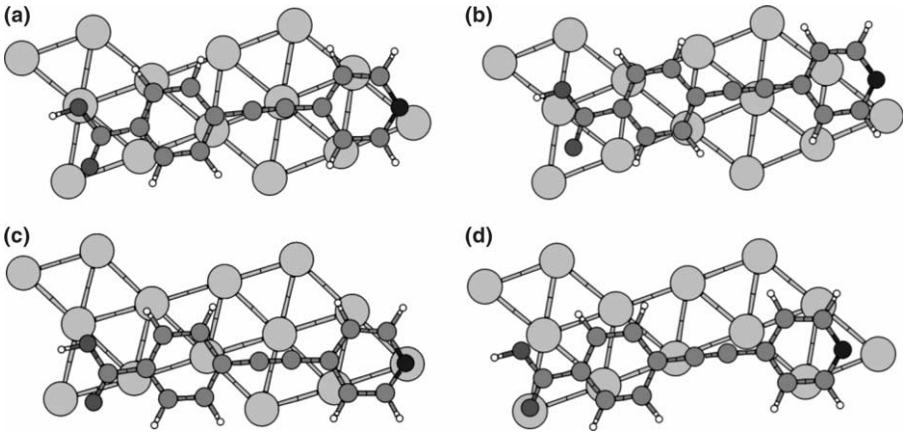

Fig. 5. Different arrangements of a PEBA molecule with respect to the surface layer used to determine the preferential adsorption site. After relaxation the structure (a) is found to be the stable one, while (b)–(d) are metastable local minima.

1.72 Å hydrogen bond, respectively. Comparing the resulting total energies with the energies of an isolated molecule in the same computational cell we obtain the corresponding energy per bond in both cases, which differ by 0.16 eV. The PEBA deformation energy: (i) due to monolayer adsorption on the surface of about 0.07 eV is calculated for an isolated molecule, keeping the atomic positions fixed as obtained after full atomic relaxation in the ML geometry. Thus the total energy cost (i, ii) is about 0.23 eV/mol/bond and is indeed less than the estimated amplitude of the adsorption potential corrugation (cf. 0.3 eV). Overall, our results indicate that the adsorption potential corrugation acts on the same energy scale as the inter-molecular interactions, in agreement with the hypothesis of adsorption-induced ML periodicity and orientation.

Some insight into the chemical interaction between the molecule and the surface can be achieved by looking at the interaction-induced differential charge density. Keeping the atomic positions fixed, we separately calculate the charge density associated to the clean silver slab and to the PEBA molecule in vacuum, and subtract them from the total charge density of the interacting system. The main feature of the resulting redistribution pattern can be interpreted as a charge transfer between the highest occupied and lowest unoccupied molecular orbitals (HOMO and LUMO, respectively), combined with a slight modification of the molecular orbitals due to the presence of the surface. Fig. 7(a) and (b) shows 2D contour plots of the charge density parallel to the surface, corresponding to cut planes placed (a) 0.7 Å above and (b) 0.7 Å below the molecule (see also Fig. 6). For comparison, we report in Fig. 8(a) and (b) the HOMO and LUMO orbitals of an isolated molecule obtained from a simple extended Hückel model. The two-lobe structure of the ethynylene bridge LUMO is reproduced by the differential density both above and below the molecule, while the depletion region corresponds to the central lobe of the HOMO orbital. The nitrogen and COOH lobes appear as well in the charge redistribution picture. The slight differences between upper and lower cross-sections in Fig. 7 are presumably due to charge distortion effects reflecting the interaction with the the surface electronic orbitals. Note also that the additional lobes on the lower section are placed just above surface atoms. The redistribution of charge on the surface of the slab is also apparent in cut planes 'belonging to the z direction (not shown), and can be interpreted as the contribution of silver d-states in the interaction with the molecular layer. The overall picture on the nature of PEBA interaction with the Ag(1 1 1) surface is that of a weak interaction, with the surface states screening the dipolar molecule. Consistent with a simple first order perturbation model in the strength of such interaction, the differential electron density reveals a mixing between HOMO and LUMO states of the molecule, as well as some charge redistribution on the metallic surface.

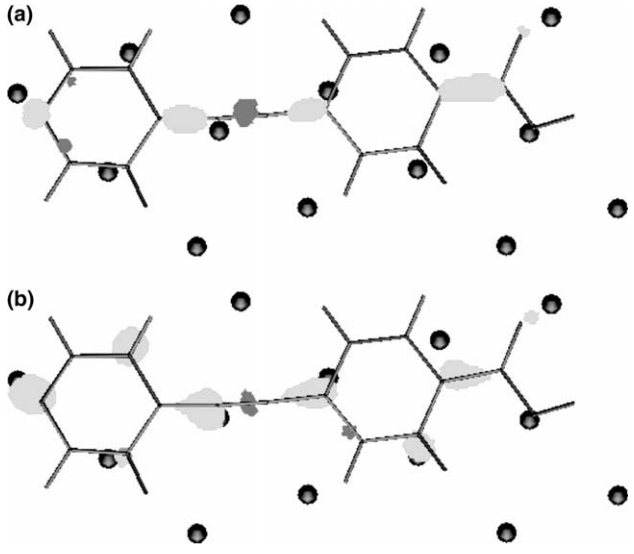

Fig. 7. Interaction-induced charge density on cut planes located 0.7 Å above (a) and below (b) the molecule (see Fig. 6). Electron density accumulation and depletion regions are shown by light and dark gray, respectively.

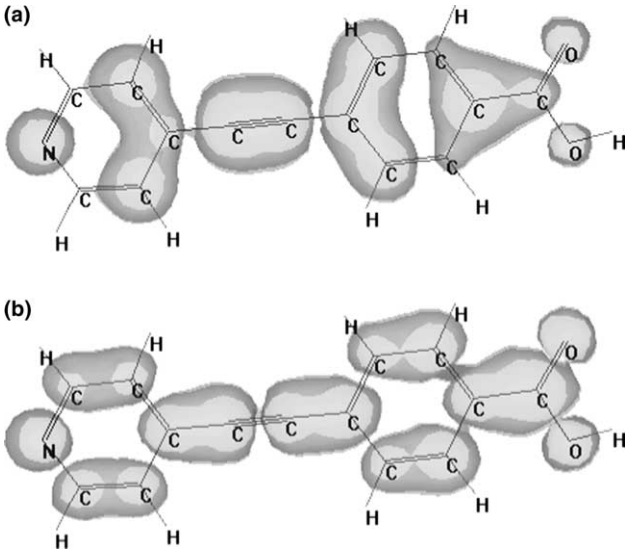

Fig. 8. HOMO and LUMO orbitals of an isolated PEBA molecule calculated using the extended Hückel model.

4. Conclusions

We presented a detailed study of PEBA adsorption on the Ag(1 1 1) substrate. The results elucidate the combined role of inter-molecular hydrogen bonding

and molecule–substrate interactions in determining the PEBA self-assembled supramolecular structures. While theoretical modeling allows us to analyze separately these different contributions by calculations on ideal structures such as the gas-phase PEBA monolayer, our calculations also reveal atomistic details of real structures which are not yet experimentally accessible. Using ab initio techniques, we determined the geometry and the energetics of the head-to-tail PEBA dimer. Modeling the gas phase PEBA ML structure and comparing the result with those of our STM observations reveals that the translational symmetry of the Ag(1 1 1) surface induces molecular stretching effects as well as significant adjustments of the OH···N bonds lengths with respect to the ideal "gas-phase" values. The estimated energy cost of these combined effects is about 0.2 eV/mol/bond. Comparing this with the strength of the interaction between molecules and substrate reveals that bonding with the surface is the determinant factor for the $[3\bar{1}\bar{2}]$ molecular orientation within the PEBA islands. Indeed, taking the silver substrate explicitly into account in a series of ab initio calculations, we estimate the amplitude of the adsorption corrugation potential to be $\leqslant 0.3$ eV/mol (note that the overall binding energy for the PEBA ML on the substrate has a much higher value, i.e., 1.56 eV/mol in the GGA approximation). We investigated the ML arrangement of the molecules as well as the preferential ML adsorption geometry on the substrate atoms. A tendency of placing oxygen atoms on top of Ag substrate atoms is apparent, while the average distance between the molecule and the substrate is found to be 2.7 Å, the pyridyl group being about 0.1 Å closer to the surface. Finally, the interaction between molecules and the substrate can be interpreted in terms of molecular orbitals hybridization effects. The nodal structure of the interaction-induced differential charge density is consistent with a simple model of first-order depletion of the filled HOMO level of the unperturbed molecule with a correspondent filling of the empty LUMO orbital. Our results substantiate that combined investigations employing STM and model simulations can provide comprehensive insight into the supramolecular ordering of functional organic species at well-defined surfaces.

Acknowledgements

We gratefully acknowledge Ch. Cai (Univ. of Houston, Texas) for providing the PEBA molecules. KK, JVB and ADV acknowledge funding from the ESF EUROCORES SONS-070 FUN-SMARTs Project.

References

[1] Böhringer M, Morgenstern K, Schneider W-D, Berndt R, Mauri F, De Vita A, et al. Phys Rev Lett 1999;83:2.
[2] Weckesser J, De Vita A, Barth JV, Cai C, Kern K. Phys Rev Lett 2001;87:096101.
[3] Hafner J. Acta Mater 2000;48:71.
[4] Jortner J, Ratner M, editors. Molecular electronics, chemistry of 21st century. Oxford: Blackwell; 1997;
Service RF. Science 2002;295:2399.
[5] Bosshard Ch, Sutter K, Prêtre P, Hulliger J, Flörsheimer M, Kaatz P, et al. Organic nonlinear optical materials. Amsterdam: Gordon and Breach; 1995.
[6] Cai C, Bösch M, Tao Y, Müller B, Gan Z, Kündig A, et al. J Am Chem Soc 1998;120:8563.
[7] Cai CZ, Müller B, Weckesser J, Barth JV, Tao Y, Bösch M, et al. Adv Mater 1999;11:750.
[8] Barth JV, Weckesser J, Cai CZ, Günter P, Burgi L, Jeandupeux O, et al. Angew Chem-Int Edit 2000;39:1230.
[9] Barth JV, Weckesser J, Trimarchi G, Vladimirova M, De Vita A, Cai Ch, et al. J Am Chem Soc 2002;124(27):7991.
[10] Limbach H-H, Manz J, editors. Hydrogen transfer: experiment and theory [Special issue]. Ber. Bunsen-Ges. Phys Chem 1998;102:289.
[11] Kamna MM, Graham TM, Love JC, Weiss PS. Surf Sci 1998;419:12;
Böhringer M, Morgenstern K, Schneider W-D, Wühn M, Wöll C, Berndt R. Surf Sci 2000;444:199.
[12] Smoluchowski R. Phys Rev B 1941;60:661.
[13] Jeffrey GA. An introduction to hydrogen bonding. New York: Oxford University Press; 1997.
[14] Perdew JP, Wang Y. Phys Rev B 1992;45:13244.
[15] Ceperly DM, Adler BJ. Phys Rev Lett 1980;40:566.
[16] Sprik M, Hutter J, Parrinello M. J Chem Phys 1996;105:1142.
[17] Brivio GP, Trioni MI. Rev Mod Phys 1999;71:231.
[18] Scoles G. private communication.
[19] Troullier N, Martins JL. Phys Rev B 1991;43:1993.
[20] Car R, Parrinello M. Phys Rev Lett 1985;55:2471.
[21] VandeVondele J, De Vita A. Phys Rev B 1999;60:13241.
[22] Vladimirova M, Stengel M, De Vita A, Baldereschi A, Böhringer M, Morgenstern K, et al. Europhys Lett 2001;56:254.
[23] Cornell WD, Cieplak P, Bayly CI, Gould IR, Merz Jr KM, Ferguson DM, et al. J Am Chem Soc 1995;117:5179.